

CFD PREDICTION OF SUBCOOLED BOILING WITH ADVANCED MECHANISTIC MODELS OF INTERFACIAL AREA TRANSPORT EQUATION

V.T. Nguyen¹, C.-H. Song² and C.T. Tran³

¹: School of Nuclear Engineering and Environmental Physics, Hanoi University of Science and Technology, No.1 Dai Co Viet Road, Hanoi, Vietnam

²: Thermal-Hydraulics Safety Division, Korea Atomic Energy Research Institute, Daedeok-daero 989-111, Yuseong, Daejeon, 305-350, Rep. of Korea

³: Vietnam Atomic Energy Institute, 59 Ly Thuong Kiet Street, Hanoi, Vietnam

thai.nguyenvan@hust.edu.vn

ABSTRACT

The capability of multiphase multidimensional CFD (Computational Fluid Dynamics) modeling of subcooled boiling phenomena and the mechanism of DNB (Departure from Nucleate Boiling) has been extensively investigated in ANSYS CFX, STAR-CD and several in-house developed codes. Mechanistic modeling of interfacial area concentration is great of importance for accurate prediction of bubble size distribution which governs interfacial heat transfer terms between two-phase. New bubble coalescence and breakup models considering turbulent suppression phenomena, which could possibly occur in high liquid velocity condition of turbulent bubbly two-phase flow, have been developed and the validation results have shown the significant improvement of bubble size distribution in adiabatic flow condition. The benchmark calculation against DEBORA data presented in this paper also confirmed the applicability of newly developed models to get a good prediction results in subcooled boiling condition.

KEYWORDS

CFD, Subcooled boiling, interfacial area concentration, suppression phenomena

1. INTRODUCTION

In the advanced two-fluid model currently used in many general computational fluid dynamic codes and more specific nuclear thermal-hydraulics analysis codes, the interfacial area concentration is a very important quantity that determines the intensity of inter-phase mass, momentum, and energy transfer. The interfacial area transport equation has been developed intensively to describe the temporal and spatial evolution of the two-phase geometrical structure in a two-phase flow [1,2]. In the interfacial area transport equation, the development of physical models for bubble coalescence and break-up source terms requires the consideration of bubble size distribution as well as the dynamic interaction between bubbles or bubble and liquid turbulence. The break-up and coalescence kernel of Prince and Blanch [3] and Luo and Svendsen [4] have been widely used in the open literature.

By assessment of previous break-up and coalescence models of Wu et al. [5], Hibiki and Ishii [6], and Yao and Morel [7], Nguyen et al.[8] pointed out that the bubble coalescence and break-up models of these models are strongly dependent upon the turbulent energy dissipation rate. Considering the turbulent enhancement phenomena in bubbly two-phase flow, they found that the implementation of bubble-

induced turbulence (BIT) models with source terms in the standard k - ϵ equations can improve the prediction results of these model under low superficial liquid velocity and high void fraction conditions.

However, the BIT approach failed to predict the bubble size under a high superficial liquid velocity condition. For these cases, the bubble sauter mean diameter is strongly underestimated and the interfacial area concentration is strongly overestimated, especially at the region close to the wall. The predicted values of turbulent kinetic energy generation and dissipation rate are very large due to a high liquid velocity gradient near the wall boundary, and they might lead to a strong overestimation of bubble break-up source term in the interfacial area transport equation.

In the previously published models for bubble break-up source term, the whole turbulent kinetic energy of single eddy was considered as the possible energy for bubble break-up process, and a fractional loss of liquid turbulent eddy energy which is converted to and maintained as surface energy due to surface distortion has not been taken into account. Moreover, the turbulent eddy scale is an important factor for two bubbles keeping in contact with each other in the beginning step of a coalescence event. Therefore, the distribution of turbulent eddy size should be taken into account in the modeling of contact time between bubbles. Based on that approach, Nguyen et al. [8] developed bubble coalescence and break-up models taking into account the turbulent suppression phenomena. The original contact time in the bubble coalescence model, which is solely derived from a dimensional analysis, was extended by selecting the turbulent eddy size as a characteristic length, and taking into account the fragmentation process of a turbulent eddy. Local measurements of bubbles such as void fraction, bubble/liquid velocities, interfacial area concentration and bubble size were performed at three axial elevations in the KAERI-VAWL test facility [9] and PURDUE test facility [10] using the conductivity probe method to have been used for validation of developed modes implemented in CFD EAGLE (Elaborated Analysis of Gas-Liquid flows Evolution) code Results from the calculation clearly show the improvements of the newly developed models. Results from the calculation clearly show the improvements of the newly developed models. This paper presented the benchmark calculation against DEBORA data (Garnier et al., 2001) that confirms the applicability of newly developed models to get a good prediction results in subcooled boiling condition. Moreover, these calculations have taken into account the temperature dependence of fluid properties (density, specific heat capacity, thermal conductivity, and viscosity) that previous studies have not considered.

2. ADVANCED MODELS FOR ONE-GROUP INTERFACIAL AREA TRANSPORT EQUATION CONSIDERING TURBULENT SUPPRESSION PHENOMENA

2.1. Turbulence suppression phenomena

Turbulent kinetic energy is one of most important variables in two-phase flow since it is a measure of turbulence intensity, which is a ratio of the root-means-square of the turbulent velocity fluctuation and the mean velocity. In the experiments of two-phase flow turbulence, one interesting phenomenon has been observed particularly in bubbly flow regime, which is "turbulence suppression". Serizawa and Kataoka (1990) and Kataoka et al. (1993) defined "turbulence suppression" as phenomena in which the local kinetic energy in a two-phase flow becomes smaller than that in a single phase flow for the same averaged liquid flux somewhere in the radial position of the pipe. In relation to the turbulence suppression, "turbulence augmentation" is defined as the phenomena in which the local turbulent kinetic energy in two-phase flow is larger than everywhere in the radial position of the pipe. The transition between turbulence suppression and turbulence augmentation is defined as the boundary where the turbulence suppression phenomenon is no more observed. Based on their experimental observations and the previously published works, a turbulence suppression/augmentation map was qualitatively obtained in a j_l - j_g diagram, where turbulent augmentation occurs in a small liquid flux, and turbulence suppression occurs in a large liquid flux (see Fig. 1)

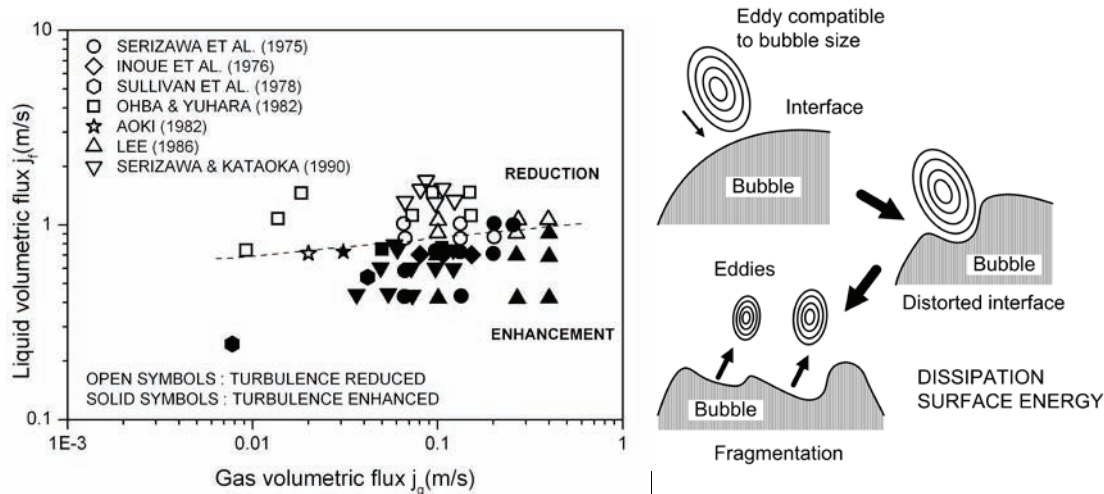
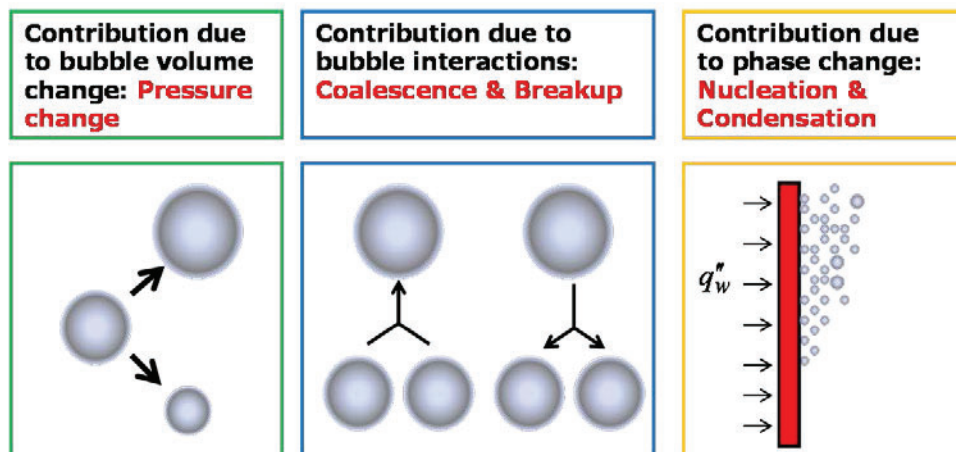


Figure 1: Turbulence suppression/ augmentation map and eddy/interface interaction model (Serizawa and Kataoka, 1990)

2.2. Break-up and Coalescence Models considering Turbulent Suppression Phenomena

The volumetric interfacial area transport equation, which can describe the temporal and spatial evolution of the two-phase geometrical structure, for a bubbly flow is given as follows:

$$\frac{\partial a_i}{\partial t} + \nabla \cdot (a_i \bar{u}_g) = \frac{2}{3} \frac{a_i}{\alpha} \left[\frac{\partial \alpha}{\partial t} + \nabla \cdot (\alpha \bar{u}_g) \right] + \frac{36\pi}{3} \left(\frac{\alpha}{a_i} \right)^2 (\phi_n^{CO} + \phi_n^{BK}) + \phi_n^{NUC} \quad (1)$$



The first term on the right hand-side of Eq. (1) is the term for a bubble size variation from a pressure drop. The second and third terms are the variance of the interfacial area concentration from the coalescence and break-up phenomena. Nguyen et al. (2013) developed bubble coalescence and break-up models taking into account the turbulent suppression phenomena. The original contact time in the bubble coalescence model, which is solely derived from a dimensional analysis, was extended by selecting the turbulent eddy size as a characteristic length, and taking into account the fragmentation process of a turbulent eddy. The details of the development process can be found in Nguyen et al. (2013) and newly developed models are summarized in Table 1 including state-of-the-art break-up and coalescence models of Wu et al. (1998), Hibiki and Ishii (2002) and Yao and Morel (2004).

Table 1: Break-up and Coalescence Models

Model	Break-up	Coalescence
	$\phi_n^{BK} = f_b \eta_b = \frac{1}{T_b} n \eta_b, \phi_n^{CO} = -f_c \eta_c = -\frac{1}{T_c} n \eta_c$	
Wu et al. (1998)	$\frac{f_b}{n \varepsilon^{1/3} / d_s^{2/3}} = \frac{1}{\alpha_{max}^{1/3} (\alpha_{max}^{1/3} - \alpha^{1/3})} \left[1 - \frac{We_{cr}}{We} \right]^{1/2}$ $\eta_b = \Gamma_{TI} \exp\left(-\frac{We_{cr}}{We}\right)$ $We_{cr} = 2.0, \alpha_{max} = 0.8, \Gamma_{TI} = 0.18, We_{cr} = 2.0$	$\frac{f_c}{n \varepsilon^{1/3} / d_s^{2/3}} = \frac{6\alpha}{\pi \alpha_{max}^{1/3} (\alpha_{max}^{1/3} - \alpha^{1/3})}$ $\times \left[1 - \exp\left(-K_{RC} \frac{\alpha_{max}^{1/3} \alpha^{1/3}}{\alpha_{max}^{1/3} - \alpha^{1/3}}\right) \right]$ $\eta_c = \Gamma_{RC}$ $\Gamma_{RC} = 0.0565, K_{RC} = 3.0, \alpha_{max} = 0.8$
Hibiki and Ishii (2002)	$\frac{f_b}{n \varepsilon^{1/3} / d_s^{2/3}} = \frac{1 - \alpha}{(\alpha_{TI,max} - \alpha)}$ $\eta_b = \Gamma_{TI} \exp\left(-K_{TI} \frac{2}{We}\right)$ $\alpha_{TI,max} = 0.741, \Gamma_{TI} = 0.021, K_{TI} = 1.59$	$\frac{f_c}{n \varepsilon^{1/3} / d_s^{2/3}} = \frac{\alpha}{(\alpha_{RC,max} - \alpha)}$ $\eta_c = \frac{\Gamma_{RC}}{2} \exp\left(-K_{RC} \sqrt{\frac{We}{2}}\right)$ $\alpha_{RC,max} = 0.741, \Gamma_{RC} = 0.0314, K_{RC} = 1.29$
Yao and Morel (2004)	$\frac{f_b}{n \varepsilon^{1/3} / d_s^{2/3}} = \frac{\pi}{6} \left[\frac{\Gamma_{TI} (1 - \alpha)}{1 + K_{TI1} (1 - \alpha) \sqrt{We/We_{cr}}} \right]$ $\eta_b = \exp\left(-\frac{We_{cr}}{We}\right)$ $\Gamma_{TI} = 1.0, K_{TI1} = 0.42, We_{cr} = 1.24$	$\frac{f_c}{n \varepsilon^{1/3} / d_s^{2/3}} = \frac{\pi}{6} \left[\frac{\Gamma_{RC} \alpha_{max}^{1/3}}{(\alpha_{max}^{1/3} - \alpha^{1/3}) + K_{RC1} \alpha_{max}^{1/3} \alpha \sqrt{We/We_{cr}}} \right]$ $\eta_c = \exp\left(-K_{RC2} \sqrt{\frac{We}{We_{cr}}}\right) K_{RC2} = 1.017, We_{cr} = 1.24$ $\Gamma_{RC} = 2.86, K_{RC1} = 1.922, We_{cr} = 1.24, \alpha_{max} = 0.52$
Nguyen et al. (2013)	$f_b = \frac{\varepsilon^{1/3}}{d_s^{11/3}} \left[\frac{\Gamma_{TI} \alpha (1 - \alpha)}{1 + K_{TI1} (1 - \alpha) \sqrt{We/We_{cr}}} \right]$ $\eta_b = \exp\left(-\frac{K_{TI2}}{(1 - c_3)} \frac{\sigma}{\rho_f \varepsilon^{2/3} d_s^{5/3}}\right)$ $\Gamma_{TI} = 1.6, K_{TI1} = 0.42, K_{TI2} = 1.59$	$f_c = \frac{\varepsilon^{1/3}}{d_s^{11/3}} \left[\frac{\Gamma_{RC} \alpha^2 \alpha_{max}^{1/3}}{(\alpha_{max}^{1/3} - \alpha^{1/3}) + K_{RC1} \alpha_{max}^{1/3} \alpha \sqrt{We/We_{cr}}} \right]$ $\eta_c = \exp\left(-\frac{K'_{RC2}}{c^{2/3}} \sqrt{\frac{\rho_c \varepsilon^{2/3} d_s^{5/3}}{\sigma}}\right)$ $\Gamma_{RC} = 2.86, K_{RC1} = 1.922, K'_{RC2} = 0.913$ $c = 11/3 \sqrt{\frac{2.24 \times (1 - c_3) (c_1^{2/3} - c_2^{2/3})}{(c_2^{-3} - c_1^{-3})}}$

The last term on the right-hand side in Eq. (1) denotes an increase in IAC by a bubble nucleation at the heated wall.

$$\phi_n^{NUC} = \pi d_w^2 \frac{N \cdot f \cdot A_w}{V_b} \quad (2)$$

where N , d_w , f , A_w , V_b are the active nucleate size density, the bubble departure diameter, bubble departure frequency, the area of heated surface and the volume of a unit cell, respectively.

3. WALL BOILING MODELLING

In boiling flow, wall heat partition models (Kurul and Podowski, 1990) describe the mechanisms of a heat transfer from the wall which consist of the surface quenching (q_q), evaporative heat transfer (q_e), and single phase convection (q_c). Accordingly, the given external heat flux (q_{tot}), applied to the heated wall is written as a sum of three parts:

$$q_{tot} = q_q + q_e + q_c \quad (3)$$

The individual components in this heat flux partitioning are then modeled as functions of the wall temperature and other local flow parameters. Eq. (3) can be solved iteratively for the local wall temperature T_W , which satisfies the wall heat flux balance. Denoting the fraction of area influenced by the bubbles as A_W , the heat flux components are given as following.

$$q_q = A_W h_Q (T_W - T_L) \quad (4)$$

$$q_e = \dot{m}_W H_{LG} \quad (5)$$

$$q_c = (1 - A_W) h_C (T_W - T_L) \quad (6)$$

$$A_W = \pi \left(a \frac{d_W}{2} \right)^2 N \quad (7)$$

Here a is the so-called bubble influence factor, which means the ratio of the area influenced by a nucleate boiling heat transfer to the projected area at a bubble departure. In the present study, The value a of 1 was used. It can be shown that the evaporation heat flux is one of the key parameters to be modelled for an accurate prediction of subcooled boiling flows. The generated vapor mass in conventional CFD codes is expressed as follows:

$$\dot{m}_W = \rho_G \frac{\pi}{6} d_W^3 f N \quad (8)$$

Bubble departure diameter

The bubble size at detachment depends on the liquid subcooling, liquid properties, the system pressure, the heat flux and the mechanical attraction of the surrounding flow. An investigation of the bubble size at detachment was performed by [Tolubinsky and Kostanchul \(1970\)](#) for water at different pressures and subcoolings. The observed dependence on the liquid subcooling at atmospheric pressure can be fitted to a correlation:

$$d_W = d_{ref} e^{\frac{T_{sat} - T_L}{\Delta T_{refd}}} \quad (9)$$

where $d_{ref} = 1.3$ mm and $\Delta T_{refd} = 53$ K

According to [Krepper et al \(2007\)](#), the values of d_{ref} and ΔT_{refd} had to be adjusted to $d_{ref} = 0.6$ mm and $\Delta T_{refd} = 45$ K to match the tests of [Bartolomej and Chanturiya \(1967\)](#) which were conducted at much higher pressures relevant under typical nuclear energy applications.

Active nucleate site density

The correlations of active nucleate site density are often expressed in the form of power laws depending on the wall superheat as:

$$N = N_{ref} \left(\frac{T_W - T_L}{\Delta T_{refN}} \right)^p \quad (10)$$

Literature investigations have shown that active nucleate site density is highly dependent on the microscale topography of the boiling surface. These information are very diverse in most boiling experiments. [Krepper and Rzehak \(2011\)](#) proposed the methodology which can determine the active nuclear site density for the case of missing detailed information on the micro surface structure by compensation with the measured temperature. The fact is that the active nucleate site density has almost no influence on liquid temperature, a small influence on the gas volume fraction but a strong influence on the wall superheat $T_W - T_{SAT}$. Based on their findings, values of $N_{ref} = 3.0 \times 10^7$ m⁻² for a pressure of 2.615 MPa and $N_{ref} = 5.0 \times 10^6$ m⁻² for a pressure of 1.46 MPa. The value of ΔT_{refN} is 10 K.

Bubble departure frequency

The bubble departure frequency f is given according to Cole (1960) as a function of the bubble departure diameter d_w

$$f = \sqrt{\frac{4g(\rho_L - \rho_G)}{3C_D d_w \rho_L}} \quad (11)$$

Heat transfer coefficient

Heat transfer coefficient which is written using the temperature wall function $T^+(y^+)$ known from Kader (1981) as

$$h_c = \frac{\rho C_p u_\tau}{T^+} \quad (12)$$

4. EXPERIMENTAL DATA AND NUMERICAL SIMULATION SETUP

In PWR operating conditions, subcooled boiling flow with high pressure (15 MPa), high heat flux (1 MW/m²), and high mass flux ($\sim 5 \cdot 10^3$ kg/s/m²) represents significant challenges for measurements. The sensor technology has not reached a level at which it is able to perform accurate local measurements in these conditions. However, the use of simulating fluids (refrigerants) can greatly relieve this burden. In the French tests DEBORA (Garnier et al.), Dichlorodifluoromethane (R12) was used as the working medium. This allows a choice of test parameters that is more convenient for the measurement compared to the water/steam system at high pressure. The same vapor/liquid density ratio can be achieved at a much lower system pressure and the same Reynolds number can be achieved at larger diameter of the heated pipe. This enables a measurement of radial profiles for gas volume fraction, temperature, liquid and gas velocities and of bubble sizes. The test section of DEBORA test facility is a vertical heated pipe of which the inner diameter is 19.2 mm. The total pipe length is 5 m and it consists of three parts axially. The first part is an unheated section with a 1 m length for the flow regulation at the inlet. The second part is a heated section with a 3.5 m length for the simulation of wall boiling, and the third part located at the top region is an unheated section with a 0.5 m length. Table 2 lists the parameters of the DEBORA tests selected for the present benchmark calculations which have the inlet liquid volumetric flux larger than 1.0 m/s.

Table 2: System parameters for the selected test cases

EXP. case	Pressure (MPa)	Mass Flow Rate (kg/m ² /s)	Wall Heat Flux (kW/m ²)	Inlet Temperature (°C)	Saturation Temperature (°C)	Inlet Velocity (m/s)
DEB01	1.46	2028	76.19	28.2	58.0	1.58
DEB02	1.46	2028	76.2	35.6	58.0	1.58
DEB03	2.615	1986	73.89	68.52	86.73	1.74
DEB04	2.615	1985	73.89	70.53	86.73	1.76

The EAGLE code has been developed at KAERI based on the two-fluid model and is aimed at a multi-dimensional analysis of a two-phase flow with the implementations of drag and non-drag forces, standard $k-\varepsilon$ turbulence model, and the interfacial area transport equation. The detailed code structure and Simplified Marker And Cell (SMAC) algorithm can be found in Bae et al. (2008) and Nguyen et al. (2012). To give a meaningful comparison between the CFD prediction and experiment, numerical uncertainty should first be estimated, especially on the grid sensitivity. In the present work, 2D equidistant grids in a cylindrical coordinate were used for the simulation of a pipe bubbly flow. Many works on grid sensitivity have been done in our previous studies (Bae et al, 2008; Nguyen et al., 2012). From our investigations, 10 x 80 grids in the radial and axial directions are chosen as the basic grid size for all cases. In the present calculations, the turbulent dispersion force model of Lahey et al. (1993), drag

force model Ishii and Zuber (1979) with drag force coefficient model of Ishii and Hibiki (2006), wall lubrication force of Antal et al. (1991) with coefficients of Yun et al. (2012), and lift force model of Tomiyama et al. (2002) are applied. These calculations have taken into account the temperature dependence of R-12 fluid properties (density, specific heat capacity, thermal conductivity, and viscosity)

5. RESULTS AND DISCUSSION

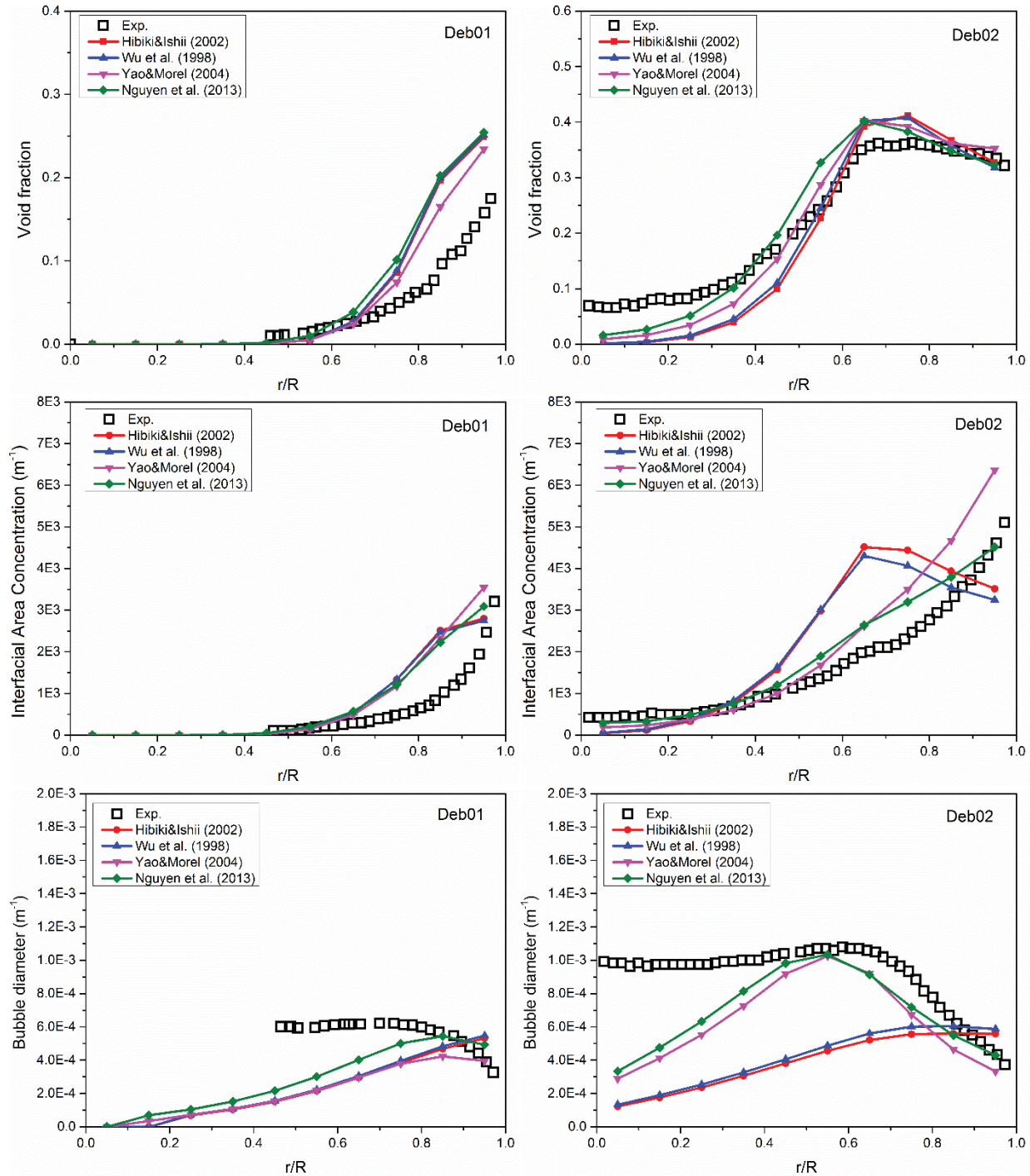


Figure 2: Comparisons of measured and calculation values for cases Deb01 and Deb02

The test cases listed in Table 2 were simulated with one-group IATE implementing bubble breakup and coalescence models in Table 1. As can be seen in Figs. 2 and 3, best agreements are obtained between experiments and calculation result in the profile the void fraction, interfacial area concentration and bubble diameter with [Nguyen et al. \(2013\)](#) breakup and coalescence models in all cases.

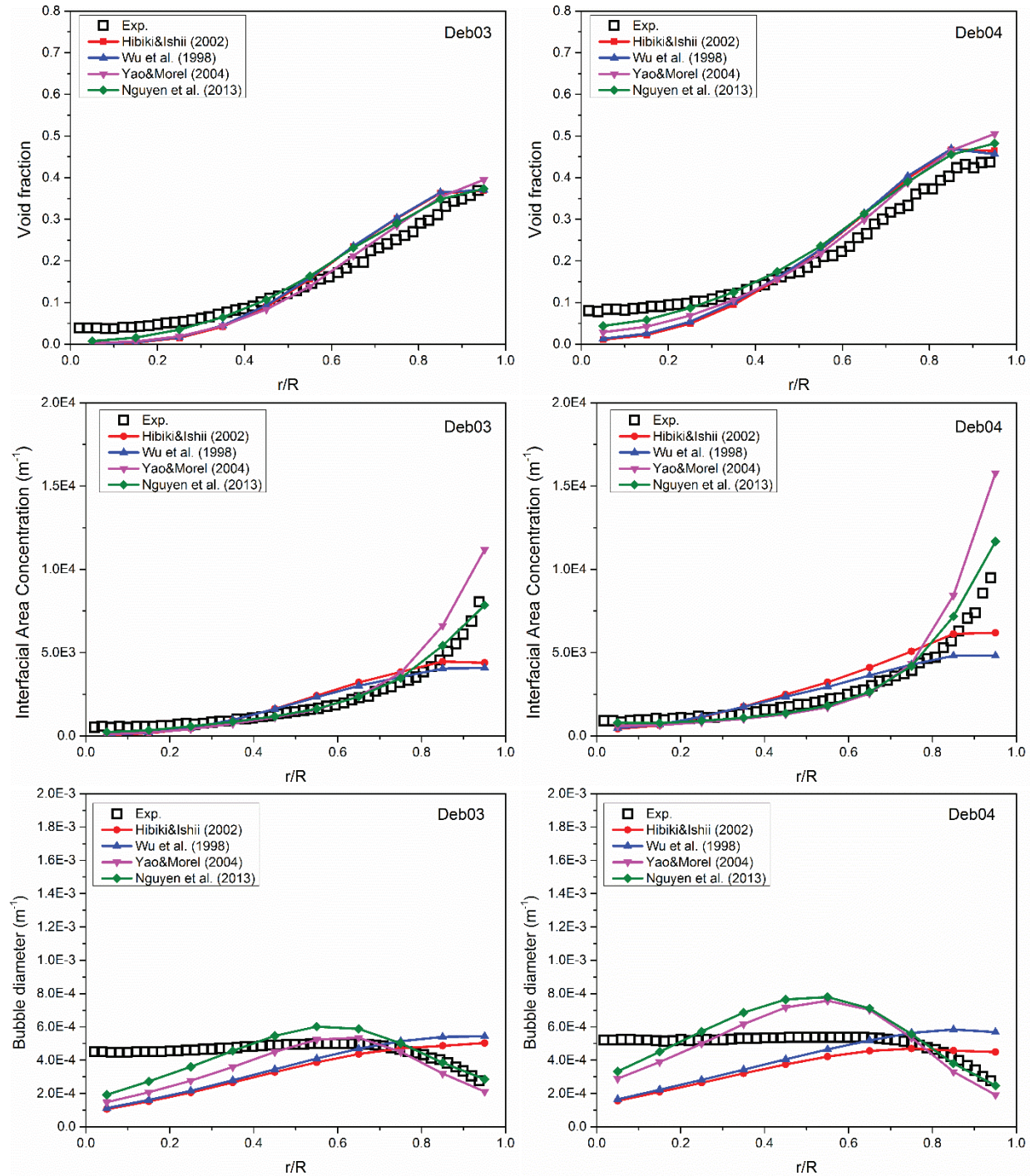


Figure3: Comparisons of measured and calculation values for cases Deb03 and Deb04

The prediction results of Yao and Morel (2004) models follow the experimental data quite well. The reason which may account for the better prediction results of Yao and Morel (2004) model compared with Wu et al. (1998) and Hibiki and Ishii (2002) models is that Yao and Morel (2004) have taken into account the free travelling time and interaction time separately. It should be noted that, the breakup and coalescence models of Nguyen et al. (2013) were developed largely based on Yao and Morel (2004) with improvement made by taking into account the turbulent suppression phenomena. In the previously published models for bubble break-up source term, the whole turbulent kinetic energy of single eddy was considered as the possible energy for bubble break-up process, and a fractional loss of liquid turbulent eddy energy which is converted to and maintained as surface energy due to surface distortion has not been taken into account. Moreover, the turbulent eddy scale is an important factor for two bubbles keeping in contact with each other in the beginning step of a coalescence event. Therefore, the distribution of turbulent eddy size should be taken into account in the modeling of contact time between bubbles.

The void fraction profile is highly affected by the non-drag forces such as lift force, wall lubrication force, and turbulent dispersion force. Krepper and Rzehak (2011) showed that the deviation observed in void fraction profile may be related to an improper balance between lift and turbulent dispersion forces and then they adjusted the strength of these forces. Yun et al (2012) also observed the high dependence of void fraction profile with largest influence of bubble lift force. They failed to achieve good prediction for the void fraction profiles of Tomiyama et al. (2002) and they used two constants with different sign according to critical bubble size. In the present calculation, lift force model of Tomiyama et al. (2002) was applied with reduction in strength by a coefficient. The strength of coefficients of lift force, turbulent dispersion force and wall lubrication force is extremely dependent on two-phase flow conditions and there is still much room for investigation on the compatibility balance of these forces.

6. CONCLUSIONS

In the present paper, bubble coalescence and breakup models considering turbulent suppression phenomena, which could possibly occur in high liquid velocity condition of turbulent bubbly two-phase flow, have been implemented in EAGLE CFD code to predict the subcooled boiling. The calculation results showed the best agreements with experiments in the profile the void fraction, interfacial area concentration and bubble diameter using our breakup and coalescence models compared with Wu et al. (1998), Hibiki and Ishii (2002) and Yao and Morel (2004) models. The benchmark calculations confirmed the applicability of newly developed models to get a good prediction results in subcooled boiling condition.

REFERENCES

1. M., Ishii, *Thermo-Fluid Dynamics Theory of Two-Phase Flow*, Eyrolles (1975)
2. M., Ishii, T., Hibiki, *Thermo-fluid dynamics of two-phase flow*, Springer Inc., New York (2006)
3. M.J., Prince, H.W., Blanch, "Bubble coalescence and break-up in air-sparged bubble columns," *AIChE J.* **36** (10), pp. 1485-1499 (1990)
4. H., Luo, H.F., Svendsen, "Theoretical model for drop and bubble break-up in turbulent dispersion," *AIChE J.* **42**, pp. 1225-1233 (1996)
5. Q., Wu, S., Kim, M., Ishii, S.G., Beus, "One-group interfacial area transport equation in vertical bubbly flow," *Int. J. Heat Mass Transfer* **41**, pp. 1103-1112 (1998)
6. T., Hibiki, M., Ishii, "Development of one-group interfacial area transport equation in bubbly flow systems," *Int. J. Heat Mass Transfer* **45**, 2351-2372 (2002)
7. W., Yao, C., Morel, "Volumetric interfacial area prediction in upward bubbly two-phase flow," *Int. J. Heat Mass Transfer* **47**, pp. 307-328 (2004)

8. V.T. Nguyen, C.-H. Song, B.U. Bae, D.J., Euh, "Modeling of bubble coalescence and break-up considering turbulent suppression phenomena in bubbly two-phase flow," *International Journal of Multiphase Flow* **54**, pp. 31-42 (2013)
9. V.T., Nguyen, D.J., Euh, C.-H., Song, "An application of the wavelet analysis technique for the objective discrimination of two-phase flow patterns," *International Journal of Multiphase Flow* **36**, pp. 755-768 (2010)
10. T., Hibiki, M., Ishii, Z., Xiao, Local flow measurements of vertical upward air-water flow in round tube. *Int. J. Heat Mass Transfer* **44**,1869-1888 (2001)
11. J., Garnier, E., Manon, G., Cubizolles, "Local measurements on flow boiling of refrigerant 12 in a vertical tube," *Multiphase Science and Technology* **13**, pp. 1-111 (2001)
12. A., Serizawa, I., Kataoka, "Turbulence suppression in bubbly two-phase flow," *Nuclear Engineering and Design* **122**, pp. 1-16. (1990)
13. I., Kataoka, A., Serizawa, D.C., Besnard, "Prediction of turbulence suppression and turbulence modeling in bubbly two-phase flow" *Nuclear Engineering and Design* **141**, pp. 145-158 (1993)
14. N., Kurul, M.Z., Podowski, "Multidimensional effects in forced convection subcooled boiling", *In: Proc. 9th Int. Heat Transfer Conf.*, Jerusalem, Israel (1990)
15. V.I., Tolubinsky, D.M., Kostanchuk, "Vapour bubbles growth rate and heat transfer intensity at subcooled water boiling," *Heat Transfer* , Preprints of papers presented at *the 4th International Heat Transfer Conference*, Paris, vol. 5, Paper No. B-2.8. (1970)
16. E., Krepper, B., Koncar, Y., Egorov, "Modelling of subcooled boiling—concept, validation and application to fuel assembly design," *Nuclear Engineering and Design* **237**, pp. 716–731 (2007)
17. G.G., Bartolomej, V.M., Chanturiya, "Experimental study of true void fraction when boiling subcooled water in vertical tubes" *Thermal Engineering* **14**, pp. 123–128 (1967)
18. E., Krepper, R, Rzehak, "CFD for subcooled flow boiling: Simulation of DEBORA experiments," *Nuclear Engineering and Design* **241**, pp. 3851–3866 (2011)
19. R., Cole, "A photographic study of pool boiling in the region of the critical heat flux," *AICHE Journal* **6**, pp. 533–542 (1960)
20. B.A., Kader, "Temperature and concentration profiles in fully turbulent boundary layers," *Int. Journal of Heat and Mass Transfer* **24**, pp. 1541-1544 (1981)
21. B.U., Bae, H.Y., Yoon, D.J., Euh, C.-H, Song, G.C., Park, "Computational analysis of a subcooled boiling flow with a one-group interfacial area transport equation," *Journal of Nuclear Science and Technology* **45** (4), pp. 341-351 (2008)
22. V.T., Nguyen, C.-H., Song, B.U. Bae, I.-C., Chu, D.J. Euh, "Simulation of DEBORA experiments for subcooled boiling flow with one-group interfacial area transport equation and the CFD EAGLE code," *Transaction of the Korean Nuclear Society Autumn Meeting*, Gyeongju, Korea (2012)
23. R.T. Lahey, Jr., Lopez de Bertodano, M., O.C. Jones, Jr., "Phase distribution in complex geometry conduits," *Nuclear Engineering and Design* **141**, pp. 177-201 (1993)
24. M., Ishii, N., Zuber, "Drag coefficient and relative velocity in bubbly flow, droplet or particulate flows," *AICHE Journal* **25**, pp. 843-855 (1979)
25. S.P., Antal, Lahey, R.T. Flaherty, J.E., "Analysis of phase distribution in fully developed laminar bubbly two-phase flow," *International Journal of Multiphase Flow* **17**, pp. 635-652 (1991)
26. B.J., Yun, A., Splawski, C.-H., Song, "Prediction of a subcooled boiling flow with advanced two-phase flow models," *Nuclear Engineering and Design* **253**, pp. 351–359 (2012)
27. A., Tomiyama, H., Tamai, I., Zun, S., Hosokawa, "Transverse migration of single bubbles in simple shear flows," *Chemical Engineering Science* **57**, pp. 1849-1858 (2002)